Journal of Sound and Vibration (2002) **250**(5), 903–921
doi:10.1006/jsvi.2001.3959, available online at http://www.idealibrary.com on IDEAL®

ANALYSIS OF STRUCTURAL ACOUSTIC COUPLING OF A CYLINDRICAL SHELL WITH AN INTERNAL FLOOR PARTITION

D. S. Li

Department of Mechanical Engineering, Laval University, Québec, G1K 7P4, Canada

L. Cheng

Department of Mechanical Engineering, The Hong Kong Polytechnic University, Hung Hom, Kowloon, Hong Kong. E-mail: mmlcheng@polyu.edu.hk

AND

C. M. Gosselin

Department of Mechanical Engineering, Laval University, Québec, G1K 7P4, Canada

(*Received* 15 *January* 2001, *and in final form* 31 *July* 2001)

In the present paper the structural acoustic coupling characteristics of a cylindrical shell with an internal floor partition are analyzed. Due to the existence of the floor, the cavity becomes irregular and both the structural and acoustic modes are difficult to express analytically. A method using "Radiation Efficiency Analysis of Structural Modes" is proposed. Typical configurations ranging from plain shells to shells with floor partitions are analyzed and, whenever possible, results are compared with those found in the literature. This method is shown to be effective when irregular-shaped cavities are involved. Meanwhile, analyses using wavenumber spectrum are also employed as an alternative. Results show that both methods have their own merit and both are very useful in the analysis of structural acoustic coupling systems, especially in the case of irregular cavities.

1. INTRODUCTION

Noise in enclosures induced by the vibration of the bounding structure is a very important issue in many engineering applications, especially in the field of aerospace and automobile engineering, where the externally excited vibrating walls of vehicles induce a significant internal sound field. This problem is very complex in nature. Due to the fact that the sound contribution from each structural mode is different, the first step towards any successful control is the identification of the most radiating structural modes by performing coupling analysis.

Constant efforts have been made by many researchers in the past several decades. Early in 1963, Lyon [1] studied the noise reduction of rectangular enclosures with one flexible wall. Then, the effect of cavities on the natural frequencies of the flexible plate was investigated by Dowell and Vass [2]. Pretlove [3, 4] showed that the effects of shallow cavities on the vibration of a plate are not negligible. Dowell *et al.* [5] proposed a general theory of structural acoustic coupling systems called acoustoelastic theory which has become the theoretical foundation for performing structural acoustic coupling analysis. Using this theory, Yarayanan [6, 7] investigated the sound transmission properties through

0022-460X/02/100903 + 19 $35.00/0

a sandwich panel into a rectangular enclosure. More recently, Pan *et al.* [8] analyzed the low-frequency acoustic response in a damped rectangular enclosure.

Another category of structures which have been widely investigated is the cylindrical shells due to the industrial need to reduce the internal noise in airplane cabins. The simplest model is an infinite or finite cylindrical shell [9–11]. Extensive research based on this model demonstrated that in the low-frequency range, which is characteristic of propeller noise, the circumferential modal response of the shell is the dominant mechanism of sound transmission. With further investigation, the effects of rings [12], stiffness [13], double walls [14] and bulkhead [15, 16] were taken into account in theoretical models. Quite recently, by considering the spatial correspondence and the frequency proximity between structural modes and acoustic modes, Henry and Clark [17] investigated the coupling of a curved panel to the interior acoustic field of a rigid-walled cylinder.

The literature review shows that due to the intrinsic complexity of the problem, much of the past research focuses on systems having regular-shaped enclosures such as a rectangular box or a plain cylindrical shell. Without doubt, these research works revealed the fundamental coupling mechanism of structure–fluid systems. However, nearly all the aforementioned works were based on the use of the so-called modal coupling coefficient. Defined as the integral of the product between a structural mode and an acoustic mode over the whole contact area, this coefficient can be easily obtained when both the structural mode and the acoustic mode can be expressed analytically, which is the case when cavities are of regular shapes. In systems involving regular-shaped cavities, a structural mode is shown to be coupled with only a few acoustic modes. Therefore, analysis using the coupling coefficient proved to be a very efficient means to perform coupling analysis. For the systems having irregular-shaped cavities, however, natural modes cannot be expressed analytically. Moreover, the selective way in which a structural mode is coupled to acoustic modes is no longer as selective. Therefore, a mode-to-mode coupling analysis becomes tedious and less relevant. In this case, a more global method is desirable to facilitate the analysis.

One of the systems which attract our attention since several years is a cylindrical shell with an internal floor. This model is used to simulate the sound field in the cabin radiated by an airplane fuselage. With the consideration of the floor, the enclosure above the floor is an irregular shaped one and hence, analytical modal solutions are not available. Despite our previous work on the free vibration and sound radiation prediction [18–20], still very little is known about the coupling characteristics for such an irregular cavity. Indeed, further coupling analysis is needed to provide us with some more meaningful guidelines for the noise control of the fuselage.

In the present paper, the structural acoustic coupling analysis of a cylindrical shell with floor is performed. The existence of the floor produces two effects on the sound field: one is its direct sound radiation, the other is its changing cavity shape from a regular one to an irregular one. Our previous work [20] has shown that when excitation is applied to the shell, the sound radiation from the floor becomes weak because of the small vibration of the floor. Therefore, the analysis of the sound radiation from the shell will be emphasized herein. Since the commonly used coupling coefficient method is not suitable here, a method named "radiation efficiency analysis of structural modes" (REASM) is proposed to analyze the coupling characteristics of the system. In addition, the floor's effect on the dispersion relationship of the shell is also discussed.

The paper is organized as follows: the vibroacoustic model and the analysis method used in the current research are outlined in section 1. In section 2, numerical results are presented and discussed. Firstly, in order to show the effectiveness of the proposed method, the coupling characteristics of a plain cylindrical shell are analyzed and compared with the results reported in the literature. Secondly, a cylindrical shell with a rigid floor is discussed.

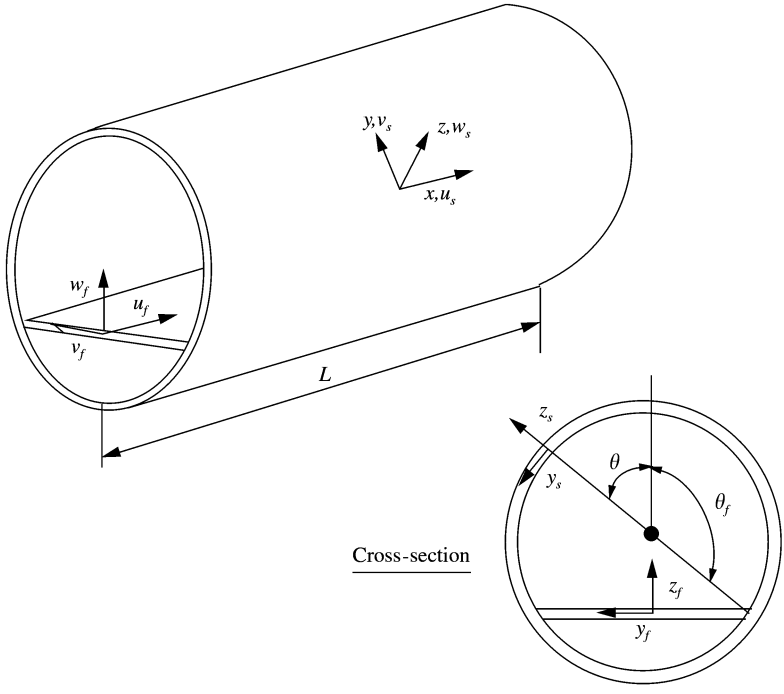

Figure 1. Structure and co-ordinate of the system.

Thirdly, the system of a cylindrical shell with a flexural floor is investigated. Finally, the floor's effect on the dispersion relationship of the shell structure is studied.

2. THEORETICAL MODEL AND ANALYSIS METHOD

The structure to be considered in the present analysis consists of a thin finite circular cylindrical shell with a longitudinal floor partition as shown in Figure 1. u_s, v_s, w_s are the longitudinal, tangential, and radial displacement of the shell and u_f, v_f, w_f the displacement of the floor in the x, y_f, z_f direction respectively. θ_f represents the position of the floor, θ is the circumferential co-ordinate of the shell and L the length of the shell. Both the shell and the floor are assumed to be homogeneous and isotropic. Structural coupling between the shell and the floor is ensured using the artificial spring system [21] for every permitted degree of freedom. The stiffness of all springs is assumed to be uniformly distributed along the two junctions. The boundary conditions of the shell–floor structure are considered simply supported at the two ends. As far as the acoustic boundary condition is concerned, the shell wall and the floor are assumed to be flexible while the two end plates are assumed to be acoustically rigid.

The theoretical model used in the present paper has been described in previous works [18–20]. The reader is referred to these works for more details. For the sake of clarity and integration, it is briefly presented here.

2.1. STRUCTURAL MODEL

The equation of motion of the structure is obtained by finding the extreme of Hamilton's function H for the structure over a suitable sub-space of displacement trial functions

expressed as follows:

$$H = \int_{t_0}^{t_1} [T_s - \Pi_s + T_f - \Pi_f - E_k + \Pi_a + E_f]\,\mathrm{d}t, \tag{1}$$

where T_s, Π_s are, respectively, the kinetic and potential energy related to the shell, T_f, Π_f are, respectively, the kinetic and potential energy to the floor, Π_a, E_f the works done by the fluid and the external mechanical loading, and E_k the strain energy stored in the artificial springs introduced at the longitudinal junctions.

The displacement vector of the shell in the longitudinal, circumferential and radial directions is decomposed as

$$\begin{Bmatrix} u_s \\ v_s \\ w_s \end{Bmatrix} = \sum_{\alpha=0}^{1} \sum_{m=1}^{\infty} \sum_{n_s=0}^{\infty} c_{mn_s}^{\alpha} \begin{Bmatrix} a_{mn_s} \cos\left(n_s\theta - \alpha\dfrac{\pi}{2}\right)\cos\left(\dfrac{m\pi x}{L}\right) \\ b_{mn_s} \sin\left(n_s\theta - \alpha\dfrac{\pi}{2}\right)\sin\left(\dfrac{m\pi x}{L}\right) \\ \cos\left(n_s\theta - \alpha\dfrac{\pi}{2}\right)\sin\left(\dfrac{m\pi x}{L}\right) \end{Bmatrix} \mathrm{e}^{\mathrm{i}\omega t}, \tag{2}$$

where (a_{mn_s}, b_{mn_s}, 1) is the modal vector of the corresponding simply supported shell with n_s and m being, respectively, the circumferential and longitudinal order. $\alpha = 0$ (or 1) means the symmetric (or antisymmetric) mode and $c_{mn_s}^{\alpha}$ is the coefficient to be determined. θ is the circumferential co-ordinate of the shell, a and L the length and the radius of the shell respectively.

For the floor, both bending and in-plane motions are expanded over the trial functions:

$$\begin{Bmatrix} u_f \\ v_f \\ w_f \end{Bmatrix} = \sum_{\alpha=0}^{1} \sum_{m=1}^{\infty} \sum_{n_f=0}^{\infty} \begin{Bmatrix} u_{mn_f}^{\alpha} \cos\left(\dfrac{n_f\pi}{b}y - \alpha\left(\dfrac{\pi}{2}\right)\right)\cos\left(\dfrac{m\pi x}{L}\right) \\ v_{mn_f}^{\alpha} \sin\left(\dfrac{n_f\pi}{b}y - \alpha\left(\dfrac{\pi}{2}\right)\right)\sin\left(\dfrac{m\pi x}{L}\right) \\ w_{mn_f}^{\alpha} \cos\left(\dfrac{n_f\pi}{b}y - \alpha\left(\dfrac{\pi}{2}\right)\right)\sin\left(\dfrac{m\pi x}{L}\right) \end{Bmatrix} \mathrm{e}^{\mathrm{i}\omega t}, \tag{3}$$

where n_f and m are, respectively, the transversal and longitudinal order. $u_{mn_f}^{\alpha}$, $v_{mn_f}^{\alpha}$, $w_{mn_f}^{\alpha}$ are the coefficients to be determined and b is the width of the floor.

It can be noted that trial functions used in both equations (2) and (3) satisfy the simply supported boundary conditions of the structures at both ends. In addition, along the shell–plate junctions, a proper assignment of the stiffness of artificial springs allows one to simulate a large variety of coupling conditions, ranging from disconnected to rigidly connected. It applies to both the displacement and the rotation. Details can be found in reference [18].

Using the expressions of the displacement of the shell and the floor, the corresponding energy and work terms in Hamilton's function can be calculated which leads to an expression in terms of the unknowns $c_{mn_s}^{\alpha}$, $u_{mn_f}^{\alpha}$, $v_{mn_f}^{\alpha}$, $w_{mn_f}^{\alpha}$. The Lagrange equation is then used to extremalize Hamilton's function and the governing equation of motion for the coupling system is obtained.

The matrix form of coupling equations can be summarized as follows:

$$\begin{bmatrix} K_{cc} & K_{cu} & K_{cv} & K_{cw} \\ K_{cu} & K_{uu} & K_{uv} & 0 \\ K_{cv} & K_{uv} & K_{vv} & 0 \\ K_{cw} & 0 & 0 & K_{ww} \end{bmatrix} \begin{Bmatrix} C \\ U \\ V \\ W \end{Bmatrix} = \begin{Bmatrix} F_s + P_s \\ 0 \\ 0 \\ F_f - P_f \end{Bmatrix}, \tag{4}$$

in which C, U, V, W include a series of unknowns related to the shell and the floor, respectively ($c^{\alpha}_{mn_s}$, $u^{\alpha}_{mn_f}$, $v^{\alpha}_{mn_f}$, $w^{\alpha}_{mn_f}$); F_s, F_f and P_s, P_f are the mechanical excitation and the acoustic loading on the shell and the floor respectively. Detailed expressions for each term can be found in reference [20]. The coupling matrix is symmetrical in which each non-zero term indicates the coupling between two different motions. More specifically, the shell's displacement is coupled to all three floor components, whilst no coupling occurs between the transverse motion and the in-plane motion of the floor.

By removing all terms on the right-hand side, equation (4) can be used to obtain the mode shapes of the structures. Note that with the unknown frequencies involved in the coupling matrix, equation (4) provides a standard eigenvalue problem. Once resolved, structural unknowns are put back into equations (2) and (3), respectively, to calculate the mode shapes. As we know, the existence of the floor does not affect the longitudinal coupling characteristics. As far as the coupling in circumferential direction is concerned, significant changes can be observed compared to the plain shell case.

2.2. ACOUSTIC MODEL

For the irregular-shaped enclosure, the integro-modal approach [19] is used to predict the internal sound pressure. The integro-modal approach is a method for analyzing the acoustic properties of irregular cavities, where it is not possible to apply the technique of separation of variables. An irregular-shaped enclosure is handled as a multi-connected cavity system, with either regular or slightly irregular sub-volumes. A virtual membrane separates each pair of adjacent sub-cavities. An integral formulation ensures global continuity of the pressure between adjacent sub-cavities by assigning a zero-mass and zero-stiffness to the membrane. The cavity is discretized into N sub-cavities of both regular and irregular shapes. The modal characteristics of regular sub-cavities are analytically available for performing sound pressure decomposition. For irregular sub-cavities, the modes of the bounding sub-cavities (called envelope) which are chosen to be of regular shape are used to perform the pressure decomposition and to obtain the Green function. In the present case, the acoustic enclosure is divided into a semi-circular sub-cavity and an irregular lower part bounded by a rectangular envelope. If the mode shapes are denoted by ϕ^k_n, the sound pressure inside each sub-cavity is calculated as follows:

$$p^k = \rho c^2 \sum_{\bar{n}} \frac{a_{\bar{n}}(t)}{\bar{\Lambda}_{\bar{n}}} \Phi^k_{\bar{n}}(r), \quad 1 \leqslant k \leqslant N, \tag{5}$$

where c is the speed of the sound and ρ the fluid density. $\bar{n}$ the modal indices of the cavity and $a_{\bar{n}}(t)$ the modal pressure amplitude to be determined, $\bar{\Lambda}_{\bar{n}} = (1/V)\sum_{k=1}^{N} \int_j (\Phi^k_{\bar{n}})^2 \, \mathrm{d}v^k$ is the generalized acoustic mass of mode order $\bar{n}$. Assuming that there is no absorbent boundary condition and that the interior noise is due to arbitrary vibrating surfaces with structural modal co-ordinates $q_m(t)$ (which is the whole set of the structural unknowns $c^{\alpha}_{mn_s}$, $u^{\alpha}_{mn_f}$, $v^{\alpha}_{mn_f}$, $w^{\alpha}_{mn_f}$). Using the acoustic boundary conditions and equation (5) with Helmholtz integral, the

linear modal acoustic equation is obtained

$$\ddot{a}_{\bar{n}} + \omega_{\bar{n}}^2 a_{\bar{n}} + \sum_{k=1}^{N} \frac{A_f^k}{V} \sum_m \ddot{q}_m^k L_{\bar{n}m}^{k,k} - \frac{A_f^{N+1}}{V} \sum_m \ddot{q}_m^{N+1} L_{\bar{n}m}^{N,N+1} = 0, \tag{6}$$

where A_f^k is the area of the vibration surface related to sub-cavity k and

$$L_{\bar{n}m}^{i,j} = \frac{1}{A_f^j} \int_{S^j} \Phi_{\bar{n}}^i(r_0) \psi_m^j(r_0) \, \mathrm{d}s^j \tag{7}$$

is the modal coupling coefficient between the structural mode of order m and the cavity mode of order $\bar{n}$.

2.3. STRUCTURE–CAVITY COUPLING EQUATION

Combining the structural model and acoustic model, a vibroacoustic model is obtained which can be written in a matrix form as follows:

$$\begin{bmatrix} \mathbf{K}_{SS}(\omega) & \mathbf{K}_{SF} \\ \mathbf{B}_{FS}(\omega) & \mathbf{A}_{FF}(\omega) \end{bmatrix} \begin{Bmatrix} \mathbf{U}^S \\ \mathbf{P} \end{Bmatrix} = \begin{Bmatrix} \mathbf{F}_{SS} \\ \mathbf{0} \end{Bmatrix}, \tag{8}$$

where $\mathbf{K}_{SS}$ is the dynamic stiffness matrix of the structural system. $\mathbf{K}_{SF}$ is the fluid–structure coupling matrix. $\mathbf{B}_{FS}$ is the matrix obtained using various coefficients of the acoustoelastic coupling. $\mathbf{U}^S$ and $\mathbf{P}$ are, respectively, the unknowns related to the structural components and acoustic vectors. $\mathbf{A}_{FF}$ contains the acoustic mass and stiffness matrices. $\mathbf{F}_{SS}$ is the vector related to the mechanical excitation force applied to the structure. Since the main concern of the present work is to analyze the structural modal coupling to the acoustic cavity, $\mathbf{F}_{SS}$ is, set as zero in the coupling analysis.

2.4. RADIATION EFFICIENCY ANALYSIS OF STRUCTURAL MODE (REASM)

The classical radiation efficiency analysis is one of the powerful analysis tools used to demonstrate the radiation properties of a structure or a structural mode in free field. It is defined as

$$\sigma = \frac{\bar{P}_s}{\bar{P}_p}, \tag{9}$$

with $\bar{P}_s$ and $\bar{P}_p$ being, respectively, the average acoustic power radiated per unit area of a vibrating surface and the average acoustic power radiated per unit area of a piston that is vibrating with the same average mean square velocity at a frequency for which the piston's circumference greatly exceeds the acoustic wavelength. In the case of cavity problem, however, the radiation power defined in such a classical way becomes the power absorbed by the cavity. The radiation efficiency defined above is no longer suitable to use in our present problem. To tackle this problem, a parameter using the acoustic energy is defined as follows:

$$\sigma = 10 \log\left(\frac{E_{ac}}{E_{st}}\right), \tag{10}$$

where E_{ac} is the acoustic potential energy in the cavity due to the vibration of the surrounding structure and E_{st} the total kinetic energy of the structure, which are defined,

respectively, by

$$E_{ac} = \frac{1}{2} \int_V \frac{p_f^2}{\rho_f c_f^2} \mathrm{d}v, \qquad E_{st} = \tfrac{1}{2} \rho_s h_s S \langle V_s^2 \rangle, \tag{11, 12}$$

with p_f, ρ_f, c_f and V being, respectively, the sound pressure, the fluid density, the sound speed and the volume of cavity, ρ_s, h_s, S and $\langle V_s^2 \rangle$, respectively, the material density, the thickness, the vibrating area and the average mean square velocity of the structure.

The radiation efficiency parameter defined in equation (10) can be applied either to the whole structure or to a particular structural mode. The latter is used in the present analysis. The natural modes of the structure are firstly obtained using the structural model without the fluid and the mechanical excitations. For each structural mode, the radiated acoustic energy into the cavity at any arbitrary frequency is calculated using equation (11). The radiation efficiency of this particular structural mode can then be calculated using equations (12) and (10). After comparing the radiation efficiency of different structural modes in the frequency range of interest, the most radiating modes can be identified. It should be noted that this analysis is conducted to show the coupling of one structural mode to the whole acoustic cavity, which is believed to give more global and relevant information than the analysis using coupling coefficients.

3. ANALYSIS AND DISCUSSIONS

Numerical results presented hereafter use the following configuration: the shell and the floor are assumed to have the same thickness of 0·0032 m, the density of material 7860 kg/m^3, the Poisson ratio 0·3, Young's modulus $2{\cdot}07 \times 10^{11}$ N/m^2, the length of the cylindrical shell 1·209 m, the radius 0·254 m, sound speed 343 m/s, air density 1·2 kg/m^3, and modal loss factor for the structure and the cavity 5×10^{-3}. The shell–floor attachment is assumed to be rigid. The position of the floor is defined by $\theta_f = 131^\circ$ (Figure 1).

Analysis are performed only in low-frequency range. The ultimate purpose is to help the implementation of active structural and acoustic technique to control the low-frequency noise and the vibration of the structure from low order modes. The conclusions drawn in this paper are, therefore, only valid in this context.

For computation purposes, the structural displacement and sound pressure decomposition have to be truncated to a finite series. The criteria are the same as those used in our previous work [20]. By a careful convergence study, the number of terms in decomposition series is determined as follows: shell: (8, 10) (longitudinal, circumferential), floor: (8,5,5) (transversal, in-plane motion in x, y), cavity: (5,5,5) (longitudinal, circumferential, radial).

As can be seen later, the proposed coupling analysis method relies on the correctness of the simulation model. The one used in the present work was experimentally validated in our previous work [20]. Basically, the cavity was formed by a steel cylinder with a floor welded to the inner shell skin. Two steel end caps were used to form the rigid acoustic boundaries. Microphones were placed inside the cavity supported by a thin tube along the cylinder centerline. The tube could rotate and be moved along the centerline to get any desired measurement point. A point force was produced by a shaker and applied on the outside of the shell surface. Accelerometers and force transducers were used to measure the structural response and the excitation force. Comparisons between predicted and measured results were performed in terms of displacement/force transfer functions and the response of the cavity. Generally speaking, the simulation model seems to be accurate to predict the general tendency of the response of the system.

TABLE 1

Acoustic modes of the plain cylindrical shell under 1000 Hz

Mode order	Frequency (Hz)	Mode order	Frequency (Hz)	Mode order	Frequency (Hz)	Mode order	Frequency (Hz)	Mode	Frequency (Hz)
(0,0,0)	0	(1,0,0)	141·9	(2,0,0)	283·7	(3,0,0)	425·6	(4,0,0)	567·4
(0,0,1)	823·1	(1,0,1)	835·3	(2,0,1)	870·7	(3,0,1)	926·6	(4,0,1)	999·8
(0,1,0)	395	(1,1,0)	419·7	(2,1,0)	486·3	(3,1,0)	580·6	(4,1,0)	691·4
(0,2,0)	655·8	(1,2,0)	671	(2,2,0)	714·6	(3,2,0)	781·8	(4,2,0)	867·2
(0,3,0)	902·4	(1,3,0)	913·5	(2,3,0)	945·9	(3,3,0)	997·7		

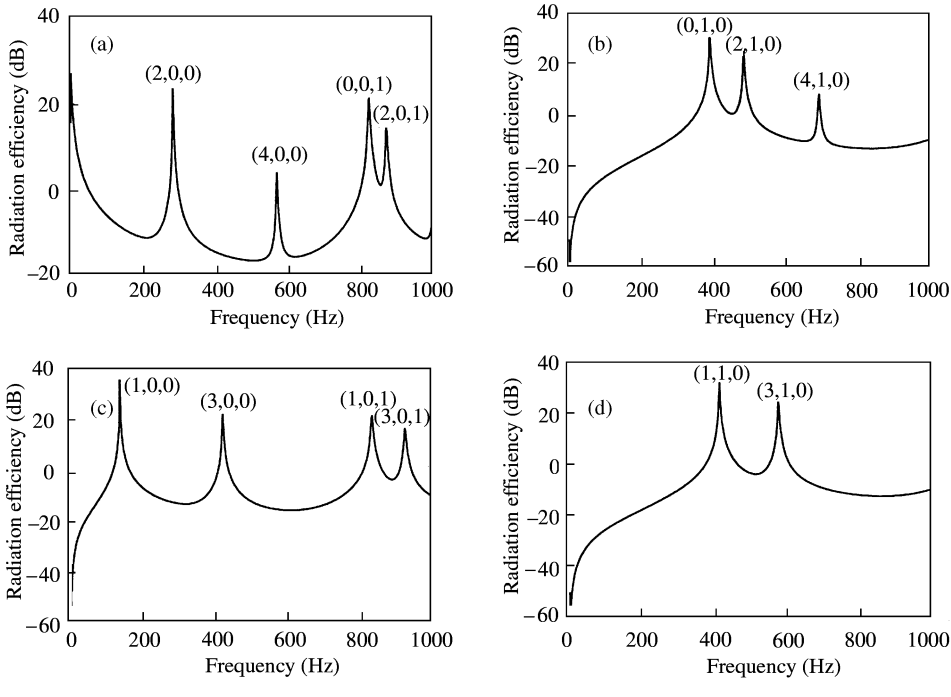

Figure 2. Radiation efficiency of natural modes of a plain cylindrical shell. (a) Structural mode (1, 0); (b) structural mode (1, 1); (c) structural mode (2, 0); (d) structural mode (2, 1).

3.1. COUPLING ANALYSIS OF A PLAIN CYLINDRICAL SHELL

A plain cylindrical shell has been extensively investigated in the literature using coupling coefficients. As a comparison basis, it is analyzed here using the REASM method. The main purpose is to show the consistency of the method and provide information that is useful for further analyses.

Table 1 tabulates all the acoustic modes of the plain cylindrical shell under 1000 Hz. Each mode is designated using three indices corresponding, respectively, to longitudinal, circumferential, and radial directions. The radiation efficiency of some typical structural modes with the longitudinal order $m = 1$ and 2 is illustrated in Figure 2. Each mode is denoted by a pair of indices representing, respectively, the longitudinal and circumferential order. In Figure 2, each peak represents one natural mode of the cavity to which the structural mode is coupled as well as the coupling intensity.

Figure 2(a) demonstrates the coupling characteristics of the structural mode (1,0) to the cavity. It can be observed that this mode is only coupled to the acoustic modes (2,0,0), (4,0,0), (0,0,1), and (2,0,1) under 1000 Hz and has the highest coupling intensity with (2,0,0). Similarly, Figure 2(b)–2(d) shows that structural mode(1,1) only couples to (0,1,0),(2,1,0); (2,0) to (1,0,0), (3,0,0),(1,0,1), (3,0,1) and (2,1) only to (1,1,0) and (3,1,0) below 1000 Hz.

These observations are consistent with the results reported in the literature. In fact, due to the perfect symmetry of the system, a structural mode is coupled to an acoustic mode in a very selective manner. This only happens when the two following conditions are satisfied: (1) both modes have the same circumferential order and, (2) their longitudinal orders are an even–odd combination pair. The coupling coefficient can be calculated using the following equation [22]:

$$B_{(u,v)(q,n,s)} = \begin{cases} \dfrac{\mathrm{J}_n(\gamma_{ns})}{2L} \dfrac{\varepsilon_n k_u (1-(-1)^{u+q})}{k_u^2 - k_q^2}, & n = v,\ (u+q)/2 \neq \text{integer}, \\ 0 & \text{otherwise}, \end{cases} \tag{13}$$

where $k_u = u\pi/L$, $k_q = q\pi/L$, $\varepsilon_n = 2$ if $n = 0$ and 1 if $n \succ 0$, with u and v being the longitudinal and circumferential order of the structural mode, respectively, q, n and s being the longitudinal, circumferential, and radial order of the acoustic mode respectively, J_n being a Bessel function of the first kind of order n, L being the length of the shell.

Compared with the coupling coefficient method which only considers the coupling between one single structural mode and one single acoustical mode, the REASM method reveals global and physical information about the coupling characteristics of a structural mode to the whole sound cavity.

3.2. CYLINDRICAL SHELL WITH A RIGID FLOOR

The floor in a cylindrical shell not only changes the regular-shaped cavity into an irregular one but also introduces coupling among modes with different circumferential orders of the shell. Both effects make the problem more complex. As pointed out before [20], the vibration of the floor is small compared to that of the shell when the excitation is directly on the shell. The floor is first assumed to be rigid to simplify the problem. The direct sound radiation from the floor is, therefore, neglected in the first step of the analysis.

Firstly, the coupling characteristics of natural modes with $m = 1$ below 600 Hz are analyzed. The radiation efficiency of these structural modes is shown in Figure 3 while the corresponding mode shapes are given in Figure 4. It can be seen from Figure 3 that each structural mode couples more or less to the same acoustic modes with different coupling intensity. Among the five modes considered, Mode 3 has the highest radiation efficiency over the overall frequency range considered, whilst Modes 4 and 5 exhibit moderate coupling strength, Modes 1 and 2 being the weakest radiators.

Further analysis is needed to understand the phenomena observed. It is well known that, in a coupled system, the fundamental factors ensuring strong coupling are the closeness of both the frequency and the waveform. In the REASM method, the frequency factor is automatically satisfied. Therefore, the waveform match between a structural mode and an acoustic mode should be the dominant factor in determining the radiation ability of the structural mode. According to the dispersion curve of sound wave in air, the low order acoustic modes have small wavenumbers. It can be anticipated that structural modes having more vibration energy component in low-wavenumber range should have higher

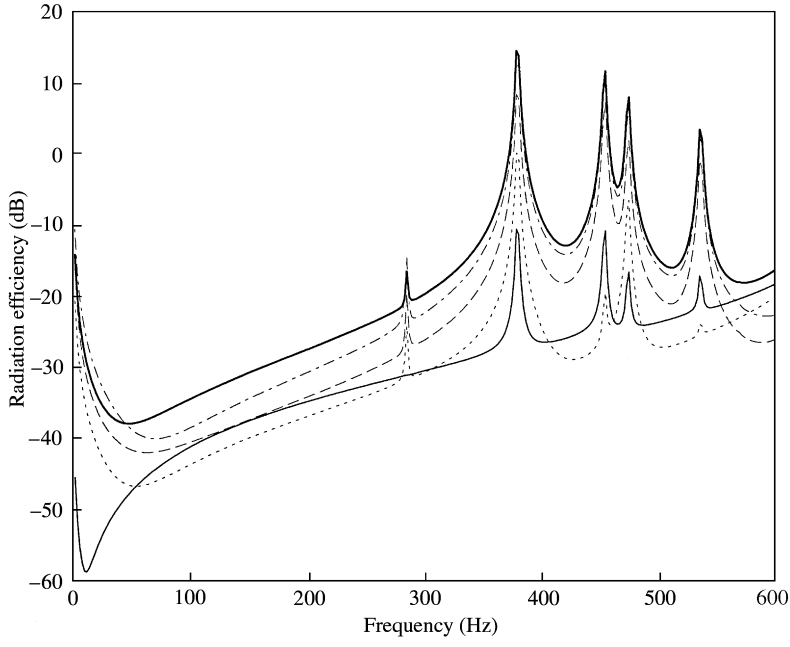

Figure 3. Radiation efficiency of natural modes ($m = 1$) of a cylindrical shell with rigid floor. ——, Mode 1; ·····, Mode 2; ———, Mode 3; –·–·–, Mode 4; – – – – –, Mode 5.

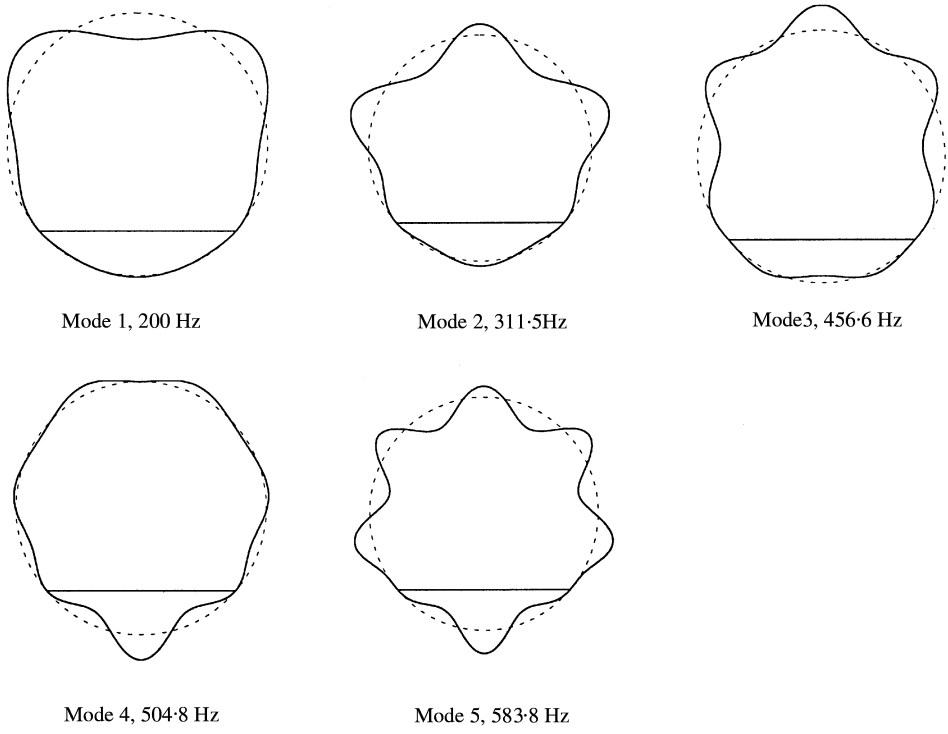

Figure 4. Mode shapes of natural modes ($m = 1$) of a cylindrical shell with rigid floor.

radiation efficiency. Due to the floor, however, the circumferential form of the structural modes is no longer regular so that the classical definition of the wavenumber is difficult to apply. Consequently, a wavenumber spectrum analysis on structural modes is performed hereafter.

In the vibroacoustic model, the radial displacement w_s is decomposed on the basis of the natural modes of the corresponding plain shell as shown in equation (2). Due to the geometry of the structure, analysis can be performed for each given α and m [18]. For $\alpha = 0$, for a given value of m, the circumferential modal shape can be expressed:

$$w_s = \sum_{n=0}^{\infty} C_{mn}^{\alpha} \cos(n\theta) \sin(m\pi x/L). \tag{14}$$

The following wavenumber transformation is then performed

$$W(k_n) = \int_{-\pi}^{\pi} w_{sc}(\theta) e^{-ik_n a\theta} \, d\theta, \tag{15}$$

where $w_{sc} = \sum_{n=0}^{\infty} C_{mn}^{\alpha} \cos(n\theta)$, k_n is the circumferential wavenumber.

Using equation (15) with equation (14) yields

$$W(k_n) = \sum_{n=0}^{\infty} C_{mn}^{\alpha} \frac{2 \sin(k_n a\pi) \cos(n\pi)}{k_n a(1 - (n/k_n a)^2)}. \tag{16}$$

The above equation can be used to plot the wavenumber spectrum of structural modes. The five modes considered previously are treated using the wavenumber transformation and the spectra in Figure 5.

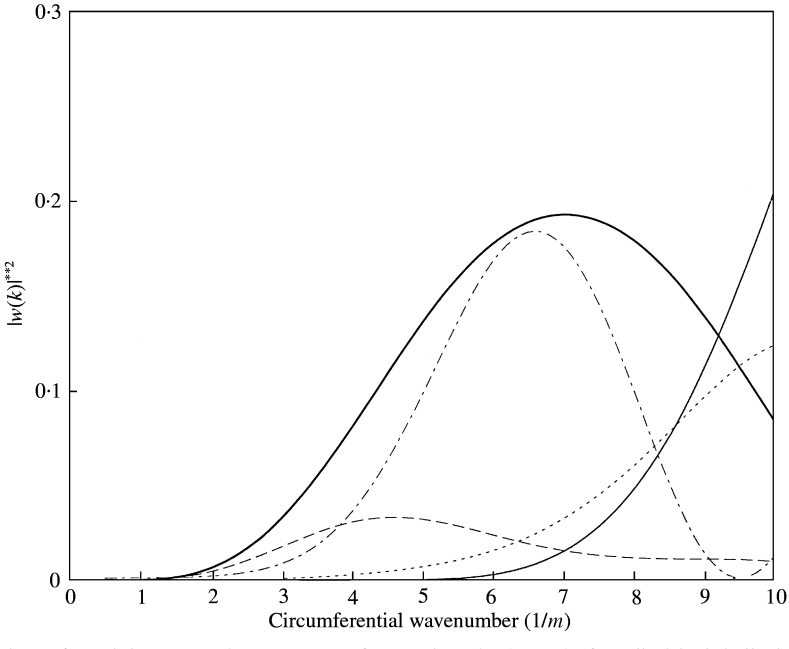

Figure 5. Circumferential wavenumber spectrum of natural modes ($m = 1$) of a cylindrical shell with rigid floor. ——, Mode 1; ·····, Mode 2; ———, Mode 3; – · – · –, Mode 4; – – – – –, Mode 5.

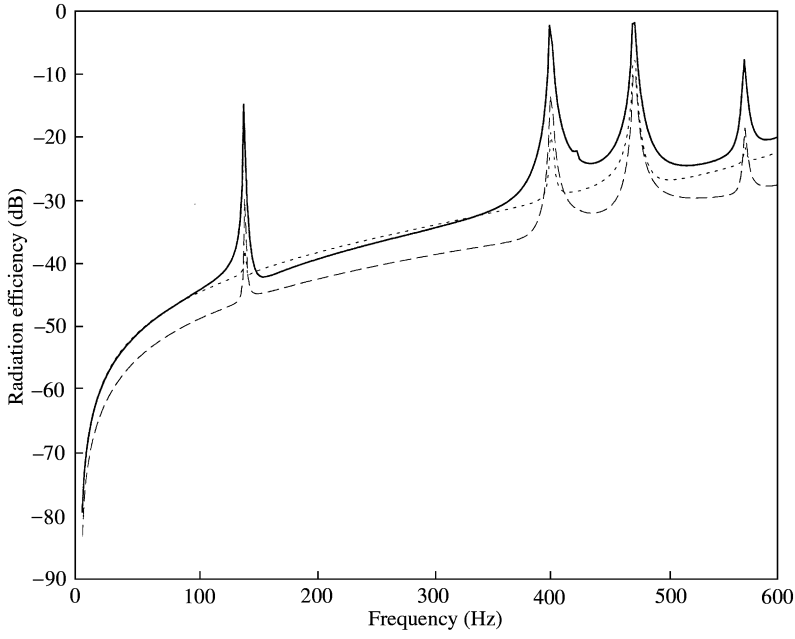

Figure 6. Radiation efficiency of structural modes ($m = 2$) of a cylindrical shell with rigid floor. – – – –, Mode 1; ·····, Mode 2; ———, Mode 3.

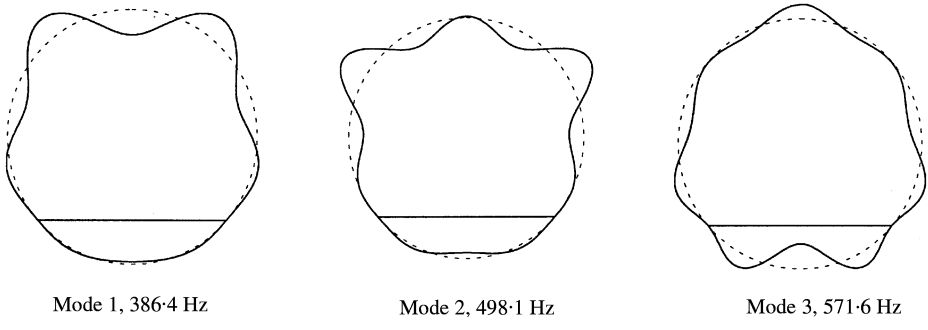

Figure 7. Mode shapes of structural modes ($m = 2$) of a cylindrical shell with rigid floor.

Since only the low order wavenumber is considered, we set the upper limit of the circumferential wavenumber to be 10. It can be observed in Table 1 that the acoustic mode (0,2,0) with a natural frequency of 655·8 Hz gives a circumferential wavenumber of 7·8 ($n/a = 2/0{\cdot}254$). Therefore, it can be approximately estimated that the circumferential wavenumbers of the acoustic modes under 600 Hz should be below 8 for the configuration considered here. Figure 5 shows that in the same wavenumber range, Mode 3 has the highest level followed by Mode 4 so that they are more effectively coupled to the cavity, leading to a higher radiation efficiency. The same analysis applies to other modes having weaker radiation efficiency. Generally speaking, the wavenumber spectrum analysis gives us conclusions similar to those drawn using the REASM method.

Using the same procedure, structural modes with $m = 2$ are also investigated with the results given in Figures 6–8. Both radiation efficiency curves (Figure 6) and wavenumber spectra (Figure 8) show that Mode 3 is a more significant sound radiator than Modes 2 and

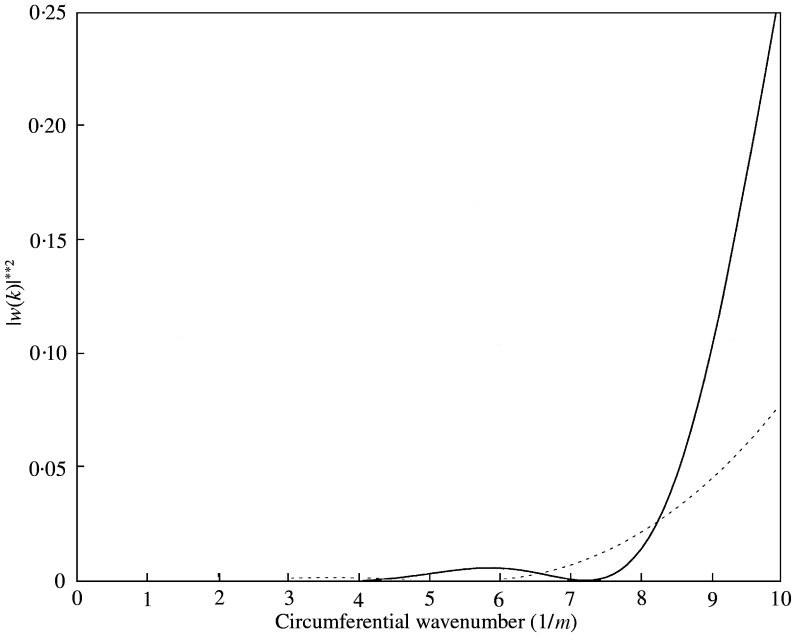

Figure 8. Circumferential wavenumber spectrum of natural modes ($m = 2$) of a cylindrical shell with rigid floor. – – – –, Mode 1; ·····, Mode 2; ———, Mode 3.

1. In fact, Mode 3 has much higher level in almost all wavenumber ranges compared to Modes 2 and 1. It should be mentioned that only two curves clearly appear in Figure 8, while the third one corresponding to Mode 2 is so close to the horizontal axis that it can hardly be noticed. Compared to the $m = 1$ case, the overall radiation efficiency of all structural modes with $m = 2$ is much smaller than that of structural modes with $m = 1$.

3.3. CYLINDRICAL SHELL WITH A FLEXURAL FLOOR

As an extension of the previous analysis, the floor is considered as flexible undergoing flexural vibrations. Figure 9 shows the first six modes with $m = 1$. It can be seen that they can be divided into three categories: shell-controlled modes for which the shell motion is more significant than that of the floor, floor-controlled modes with a strong floor motion and coupling modes with the shell and the floor vibrating in the same order of magnitude. A more accurate means of quantifying the type of the mode is to compare the average mean square velocity of the shell and the floor. Within the six given modes, Mode 1 is a floor-controlled mode, with the average mean square velocity of the floor being nearly 20 dB more than that of the shell. The five others all involve significant shell motion and will hence be emphasized in the analysis performed hereafter.

The radiation efficiencies of these modes are given in Figure 10. Similar to the case with rigid floor, all structural modes couple more or less to the same acoustic modes. It can be seen that Modes 3 and 4 have the highest radiation efficiency and all other are less efficient in sound radiation.

Again, using wavenumber transformation, the wavenumber spectrum of these structural modes are given in Figure 11. The fact that Mode 3 has the highest level in low-order wavenumber range is consistent with the observation made using Figure 10. However, it

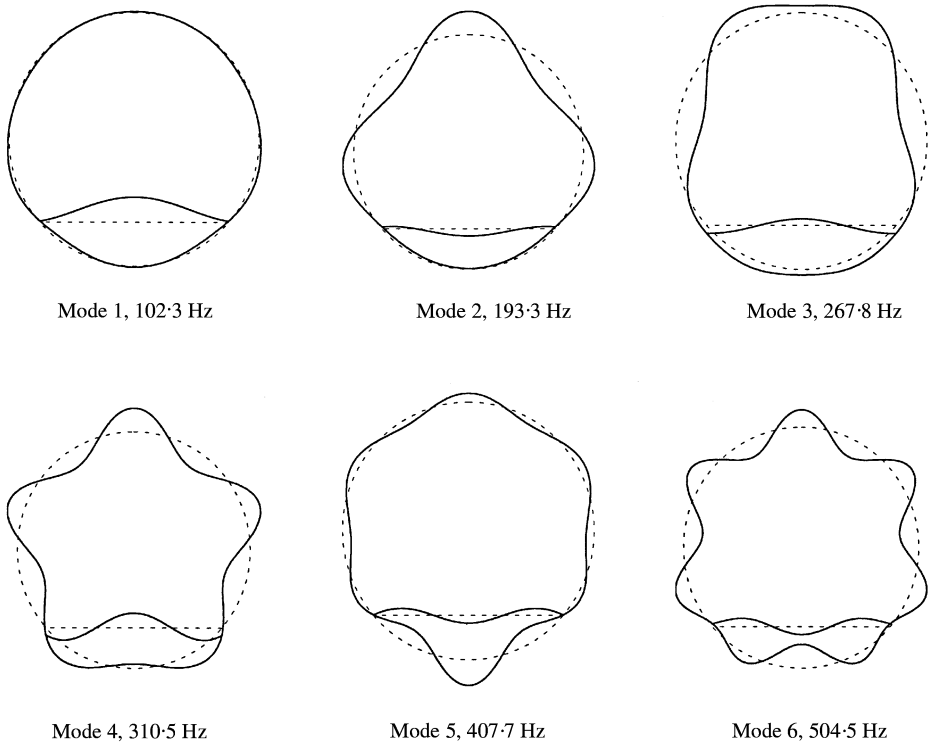

Figure 9. Structural mode shapes of a cylindrical shell with flexural floor ($m = 1$).

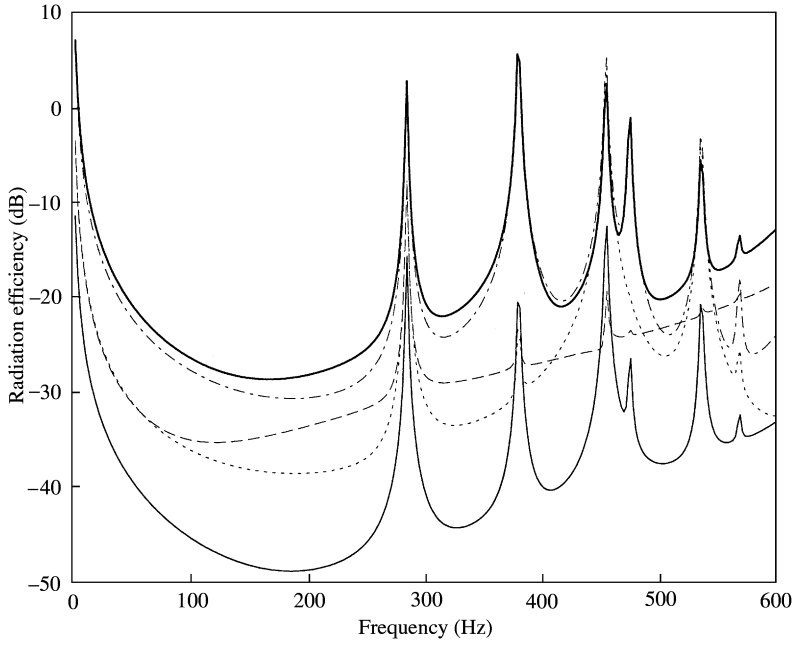

Figure 10. Radiation efficiency of shell-controlled modes ($m = 1$) of cylindrical shell with flexural floor. – – – –, Mode 2; ——, Mode 3; –·–·–, Mode 4; ———, Mode 5; ·····, Mode 6.

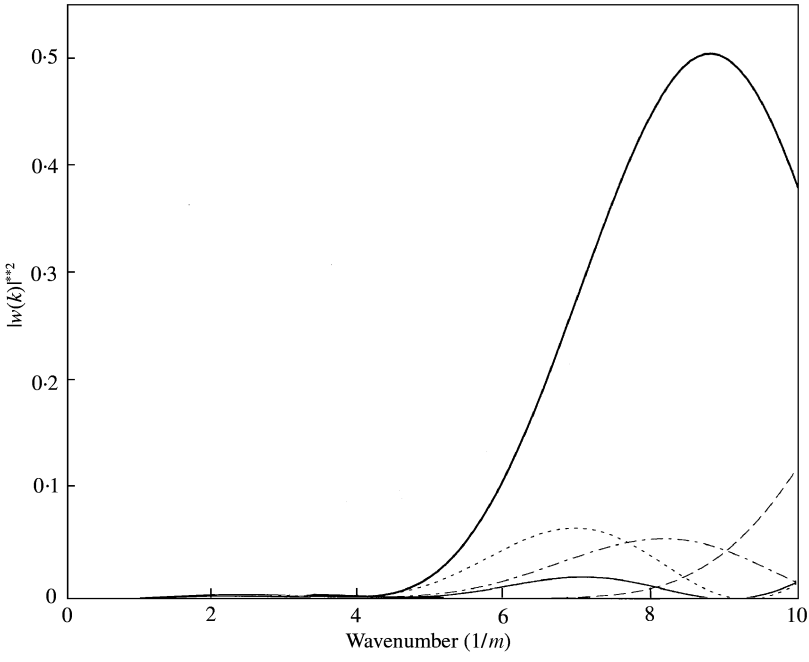

Figure 11. Circumferential wavenumber spectrum of shell-controlled modes ($m = 1$) of a cylindrical shell with flexural floor. – – – – –, Mode 2; ———, Mode 3; – · – · –, Mode 4; ·····, Mode 5; ——, Mode 6.

should also be noticed that the wavenumber spectrum would predict a much weaker radiation from Mode 4, whilst the analysis using the REASM method shows a similar level as Mode 3. This example shows the limit of the wavenumber approach, which is worth mentioning. In fact, in the present case, three factors could affect the radiation efficiency of the shell-controlled modes: the first is its vibration components in low-order wavenumber range, the second is the structural coupling intensity between the shell and the floor, the third is the radiation capability of the floor itself. Only if the three factors are considered together is it possible to obtain a satisfactory explanation for the different radiation efficiency of shell-controlled modes. The fact that the wavenumber analysis does not consider radiation from the floor and that it estimates the coupling in a very approximate way leads to less reliable results in some cases. However, due to its simplicity (only structural mode shapes are needed) it provides an interesting alternative to the whole coupling analysis, which is much more demanding in terms of analysis.

Although not shown here, analysis were also performed using structural mode with higher longitudinal orders. Again, it was noticed that the radiation efficiency of structural modes decreases when the longitudinal wavenumber increases.

3.4. EFFECT OF THE FLOOR ON THE DISPERSION RELATIONSHIP OF THE SHELL

Dispersion curves can be of great interest in understanding the interaction between waves in coupled media. Therefore, to further understand the floor effect on the structural acoustic coupling system, the dispersion relationship is investigated here.

For a plain cylindrical shell, the wavenumber is calculated by

$$k_{mn} = \sqrt{\left(\frac{m\pi}{L}\right)^2 + k_n^2}, \tag{17}$$

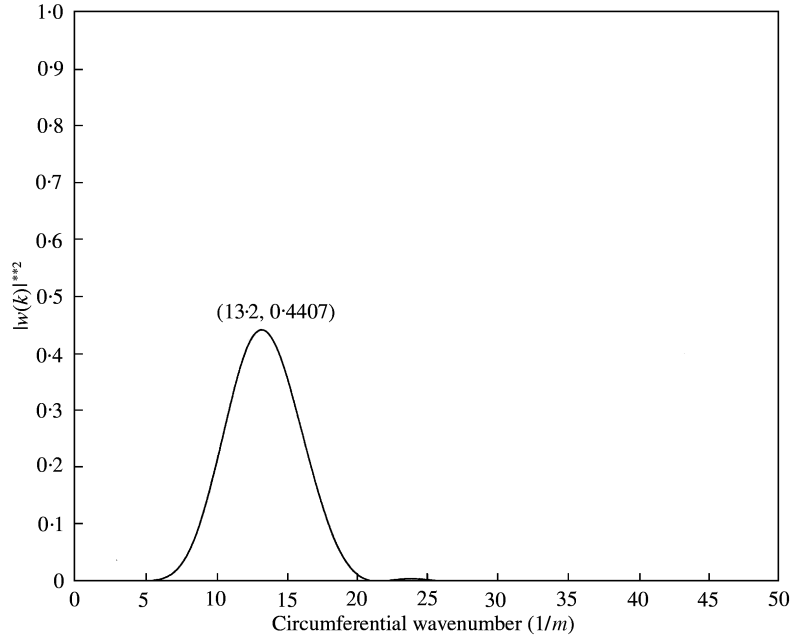

Figure 12. Circumferential wavenumber spectrum of Mode 1 ($m = 1$) of a cylindrical shell with rigid floor.

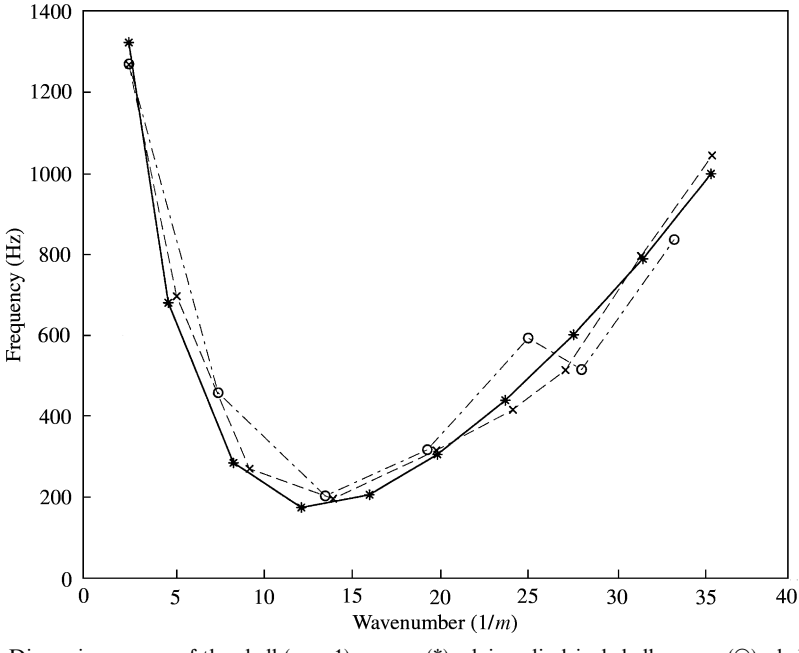

Figure 13. Dispersion curves of the shell ($m = 1$). ——— (*), plain cylindrical shell; – · – · – (○), shell with rigid floor; – – – – – (+), shell with flexural floor.

where k_{mn} is the wavenumber, the first term is the longitudinal wavenumber component with m being the longitudinal modal order and L being the length of the shell, and the second term $k_n = n/a$ is the circumferential wavenumber component with n being the circumferential modal order and a being the shell radius.

For a shell with an internal floor partition, the longitudinal wavenumber component is the same as that of a plain cylindrical shell. However, the circumferential wavenumber component is more difficult to determine because of the existence of the floor. To tackle this problem, a wavenumber transformation can be performed using equation (16). The circumferential wavenumber at which the maximum vibration component occurs is used to approximately represent the circumferential wavenumber of the structure. For example, Figure 12 shows the wavenumber spectrum of Mode 1 of a cylindrical shell with rigid floor and we can identify the approximate circumferential wavenumber component as 13·2.

Similarly, the approximate circumferential wavenumbers of other modes of a cylindrical shell with rigid floor and flexural floor are identified using the wavenumber transform method. This is then used in equation (17) to obtain the wavenumber of every structural mode. To facilitate the comparison, the dispersion curves of the shell in the three cases are plotted in a common graph as shown in Figure 13. It should be pointed out that in the case of a flexural floor, only the shell-controlled modes and the coupling modes are considered in this figure.

It can be seen from Figure 13 that the general trend is basically the same for all three cases. This observation provides justifications for the work using a plain cylindrical shell as a simplified model in noise control inside airplane fuselage structures. In the case of a rigid floor, the dispersion curve has more noticeable discrepancy from that of a plain cylindrical shell than in the case of a flexural floor. It means that with the increasing of the floor stiffness, the floor effect on the dispersion relationship of the shell structure becomes more significant. Furthermore, it could lead to an apparent change of the structural acoustic coupling characteristics which has been shown before.

4. CONCLUSIONS

The structural acoustic coupling between a cylindrical shell with a floor partition with the confined acoustic enclosure was investigated in this paper. The objective of this research was to achieve a better understanding of the physical system and provide guidelines for the noise and vibration control. A method using the "Radiation Efficiency Analysis of Structural Modes" (REASM) was proposed. This method was shown to be effective when irregular-shaped cavities are involved. Typical configurations ranging from plain shells to shells with floor partitions were analyzed and, whenever possible, results were compared with those found in the literature. Meanwhile, analyses using wavenumber spectrum were also employed. Finally, the floor effect on the dispersion relationship of the shell was discussed. The main conclusions can be drawn as follows:

(1) For a cylindrical shell with a floor, the coupling in the longitudinal direction is the same as a plain cylindrical shell. In the circumferential direction, however, a structural mode can be coupled with many acoustic modes with different circumferential wavenumbers at the same time. In the low-frequency range, structural modes with large low wavenumber components have most likely stronger noise radiation ability.
(2) In both cases of rigid floor and flexural floor, the radiation efficiency of structural modes decreases when the longitudinal wavenumber increases.
(3) Although the existence of the floor affects the dispersion relationship of the shell structure, the general trend is basically the same as a plain cylindrical shell as far as the shell portion is concerned.
(4) Two alternatives are provided when the calculation of the classical coupling coefficient becomes difficult. Due to its simplicity, the wavenumber analysis can be used as a rough

estimation of the coupling analysis. The method using the radiation efficiency analysis of structural modes (REASM) is a better tool for the structural acoustic coupling analysis. Compared to the wavenumber analysis, it takes the whole acoustic properties of the cavity into account. Compared to the coupling coefficient method, it gives information on how a structural mode can be coupled to the whole cavity. In the case of an irregular cavity in which the coupling coefficient between structural and acoustic modes is difficult to obtain and the coupling becomes more complex, it shows great merits.

ACKNOWLEDGMENTS

This work was supported by National Science and Engineering Research Council of Canada. It also partially benefited from a grant from The Hong Kong Polytechnic University (Project No. G-T280).

REFERENCES

1. R. H. LYON 1963 *Journal of the Acoustical Society of America* **35**, 1791–1799. Noise reduction of rectangular enclosures with one flexible wall.
2. E. H. DOWELL and H. M. VOSS 1963 *American Institute of Aeronautics and Astronautics Journal* **1**, 476–477. The effect of a cavity on panel vibration.
3. A. J. PRETLOVE 1965 *Journal of Sound and Vibration* **2**, 197–209. Free vibration of a rectangular panel backed by a rectangular cavity.
4. A. J. PRETLOVE 1966 *Journal of Sound and Vibration* **3**, 252–261. Forced vibration of a rectangular panel backed by a closed rectangular cavity.
5. E. H. DOWELL, G. F. GONNAN III and D. A. SMITH 1977 *Journal of Sound and Vibration* **52**, 519–542. Acoustoelasticity: general theory, acoustic natural modes and forced response to sinusoidal excitation, including comparisons with experiment.
6. S. YARAYANAN and R. L. SHANBHAG 1981 *Journal of Sound and Vibration* **74**, 453–473. Acoustoelasticity of a clamped sandwich panel backed by a cavity.
7. S. YARAYANAN and R. L. SHANBHAG 1981 *Journal of Sound and Vibration* **77**, 251–270. Sound transmission through elastically supported sandwich panels into a rectangular enclosure.
8. J. PAN, S. J. ELLIOTT and K. H. BAEK 1999 *Journal of Sound and Vibration* **223**, 543–566. Analysis of low frequency acoustic response in a damped rectangular enclosure.
9. L. R. LOVAL 1976 *Journal of Sound and Vibration* **48**, 265–275. On sound transmission into a thin cylindrical shell under flight conditions.
10. C. R. FULLER 1986 *Journal of Sound and Vibration* **109**, 141–156. Analytical model for investigation of interior noise characteristics in aircraft with multiple propellers including synchrophasing.
11. D. A. BOFILIOS and C. S. LYRINTZIS 1991 *American Institute of Aeronautics and Astronautics Journal* **29**, 1193–1201. Structure-borne noise transmission into cylindrical enclosure of finite extent.
12. B. LAULAGENT and J. L. GUYADER 1990 *Journal of Sound and Vibration* **138**, 173–191. Sound radiation by finite cylindrical ring stiffened shell.
13. M. T. CHANG and R. VAICAITIS 1982 *Journal of Sound and Vibration* **85**, 71–83. Noise transmission into semi-cylindrical enclosures through discrete curved panels.
14. E. H. DOWELL 1980 *Journal of Aircraft* **17**, 690–699. Interior noise studies for single and double walled cylindrical wall.
15. L. CHENG and J. NICOLAS 1992 *Journal of the Acoustical Society of America* **91**, 1504–1513. Radiation of sound into a cylindrical enclosure from a point-driven end plate with general boundary conditions.
16. L. CHENG 1994 *Journal of Sound and Vibration* **174**, 641–654. Fluid-structural coupling of a plate-ended cylindrical shell vibration and internal sound field.
17. J. K. HENRY and R. L. CLARK 1999 *Proceedings of ACTIVE* 99, *December* 04–06, 423–434. Structural acoustic control of a cylindrical enclosure: analysis of structural acoustic coupling.
18. J. MISSAOUI, L. CHENG and M. J. RICHARD 1996 *Journal of Sound and Vibration* **190**, 21–40. Free and forced vibration of a cylindrical shell with a floor partition.

19. J. MISSAOUI and L. CHENG 1997 *Journal of the Acoustical Society of America* **101**, 3313–3321. A combined integro-modal approach for prediction acoustic properties of irregular-shaped cavities.
20. J. MISSAOUI and L. CHENG 1998 *Journal of Sound and Vibration* **215**, 1165–1179. Vibroacoustic analysis of a finite cylindrical shell with internal floor partition.
21. L. CHENG 1996 *Shock and Vibration* **3**, 193–200. Vibroacoustic modelling of mechanically coupled structures: artificial spring technique applied to light and heavy medium.
22. S. D. SNYDER and C. H. HANSEN 1994 *Journal of Sound and Vibration* **170**, 451–472. The design of systems to control actively periodic sound transmission into enclosed spaces. Part II: mechanisms and trends.